



ELSEVIER

Optical Materials 17 (2001) 379–386



www.elsevier.com/locate/optmat

Waveguide writing in chalcogenide glasses by a train of femtosecond laser pulses

O.M. Efimov^a, L.B. Glebov^a, K.A. Richardson^a, E. Van Stryland^a,
T. Cardinal^{b,*}, S.H. Park^c, M. Couzi^d, J.L. Brun el^d

^a School of Optics, Center for Research and Education in Optics and Lasers, University of Central Florida, Orlando, FL 32816, USA

^b Institut de la Chimie de la Mati re Condens e de Bordeaux, UPR 9048, CNRS Universit  Bordeaux I, Av. du Dr. A. Schweitzer, 33608, Pessac C dex, France

^c Department of Physics, Yonsei University, Seoul, South Korea

^d Laboratoire de Physico-Chimie Mol culaire, CNRS, Universit  Bordeaux I, UMR 5803, 33405, Talence C dex, France

Received 1 May 2000; received in revised form 17 January 2001; accepted 5 February 2001

Abstract

Waveguide writing using a train of femtosecond laser pulses at 850 nm, in the transparent spectral region of bulk $\text{As}_{40}\text{S}_{60}$ glasses is reported. Waveguides were written by translating the glass sample along the optical axis of a strongly focussed laser beam. Refractive index variation, linear absorption spectra, and Raman spectra of the exposed region were measured. The chemical mechanism responsible for the index variation has been correlated to a breakage of the glass' As–S bonds and formation of As–As and S–S bonds and increase of the “disorder” of the glass network. The nonlinear optical origin leading to this phenomenon has been shown, and possible mechanisms are discussed. © 2001 Elsevier Science B.V. All rights reserved.

Keywords: Chalcogenide; Glass; Photo-induced; Waveguide writing; Raman

1. Introduction

Recent publications have proposed the possibility of a refractive index change by femtosecond laser exposure of glasses in their transparent spectral region [1–3]. Most of them have reported this effect in silica or germanosilicate glasses [1]. Recently, waveguide writing has been achieved by generating line damage inside various glasses and especially in chalcogenide ones [2]. Self-written

waveguides have also been reported in $\text{As}_{40}\text{S}_{60}$ glass films using a femtosecond 800 nm source propagating through the films axis [3]. Controlled writing of waveguides in condensed media based on modification of the optical material properties by laser irradiation may have important implications for example in optical interconnects for high data-rate optical communication systems and integrated optical elements. The ability to arbitrarily write permanent waveguides into bulk structures could be very promising in terms of fabrication of integrated optical devices and three-dimensional architecture of such devices.

Photo-induced phenomenon has been widely investigated in amorphous materials. Chalcogenide

* Corresponding author. Tel.: +33-55684-2650; fax: +33-55684-6634.

E-mail address: cardinal@icmcb.u-bordeaux.fr (T. Cardinal).

glasses are well known to exhibit reversible photo-induced effects to band gap light exposure [4–8]. The low optical band gap of chalcogenide glasses make them highly sensitive to visible exposure. Exposure to band gap wavelength light induces a photo-darkening in $\text{As}_{40}\text{S}_{60}$ glasses, a reduction of the glass band gap, and a refraction index change in the exposed region according to Kramers–Kronig relation. An important aspect of the photo-darkening is that it was not observed in crystalline materials but only in disordered materials, leading to the conclusion that photo-darkening effects are related to the increase of randomness of the glass network [9].

A correlation between reversible photo-induced effects and structural change has been discussed by different authors [8,10–13] for bulk and well annealed thin film materials. The increase of homopolar As–As and S–S chemical bonds, and of the disorder of the glass network was considered to contribute to the photo-darkening effect. Nevertheless the relation between structural change and photo-darkening is not well established.

We report permanent waveguide writing in $\text{As}_{40}\text{S}_{60}$ glasses using a train of femtosecond laser pulses. An index variation correlated to photo-darkening is shown. Micro-Raman spectroscopy has been used to show the local chemical change associated with the refractive index variation. Similarities in glass structural modification are discussed for different exposure wavelengths. Two possible mechanisms of nonlinearity are considered as the origin of the writing process.

2. Experimental

Two kinds of glass samples were used for waveguide writing: commercial high purity $\text{As}_{40}\text{S}_{60}$ glasses and glasses of $\text{As}_{40}\text{S}_{60}$ fabricated by a distillation process. The commercial samples, depending on the lot, exhibited regions with dark particles observed by optical microscopy. These dark particles were identified as carbon particles by FTIR spectroscopy, through measurement of an optical vibration spectrum at 1500 cm^{-1} characterizing the C–S bonds. In order to improve the optical quality of glasses by removing potentially

absorptive inclusions, a distillation procedure was established.

The fabrication procedure employed to obtain inclusion-free bulk glass material was the following. All the samples were fabricated in sealed fused quartz tubes under vacuum. To limit moisture contamination of the tube, the glassware was baked at $900\text{--}1000^\circ\text{C}$. 10 g of high purity raw materials (Cerac 99.999%) were kept in a glove box under N_2 atmosphere. For the distillation step the raw materials were introduced in one side of a 70 cm long tube (outside diameter and wall thickness were 19 and 2 mm, correspondingly). The tube was then closed under vacuum with a torch (methane, oxygen) and placed in a two-zone furnace. The side of the tube containing the arsenic and sulfur was heated slowly up to 600°C to evaporate the raw material relative to the respective vapor pressure of sulfur and arsenic. The other side was kept below 100°C to allow condensation of the vapor phase materials. The distillation process took 6 h. The side of the quartz tube containing the purified material was then separated with the torch, and the sealed ampoule was ready for melting. The tube was introduced into a rocking furnace at room temperature, and the mixture was heated up to $600\text{--}700^\circ\text{C}$ and rocked for 12 h. The melt was air-quenched by removing the tube from the furnace. This procedure resulted in a reduction in the content of carbon particles contained in the bulk samples. No carbon particles could be seen by optical microscopy and no vibration bands could be seen in the IR spectra at 1500 cm^{-1} . All glasses were cut and polished to obtain square cross-section bars $5\text{ mm} \times 5\text{ mm} \times 15\text{ mm}$.

The train of 100 fs laser pulses used to write the waveguide structures in this study was generated by a Ti:sapphire laser at a wavelength of 850 nm and a repetition rate of 80 MHz. An average power of up to 0.32 W was used, or 4 nJ per pulse. The beam was focused into the bulk of glass samples with spot sizes ranging from 2 to 10 μm . To record the waveguides the samples were translated along the optical axis of focusing system at a constant rate of $\cong 0.1\text{--}0.6\text{ cm/s}$. Optical micrographs of the resulting waveguides were recorded using a Nikon Labophot-2A optical microscope equipped with

a high resolution camera with Hitachi KPD50 1/2" color CCD.

To evaluate the refraction index variation between the waveguide (exposed region of the glass sample) and the cladding (unexposed region), the optical setup shown in Fig. 1 was used. The beam of a 632.8 nm He–Ne laser was expanded using a telescope (1) up to the size which provided a homogeneous distribution of irradiance along the aperture of the objective (2). This objective with diameter and focal length of 50 mm, focussed the laser radiation onto the front surface of the sample (3), at the waveguide entrance. The objective (4) was used to transfer the image exit surface of the waveguide from the back surface of the sample onto a screen (5). A diaphragm (6) of ~ 2.5 mm in diameter was placed in front of the objective (2) and could be moved along its diameter. This allowed to change the input angle of the laser at the waveguide entrance, to examine the finite angular region of the waveguide, and to evaluate the variation of refractive index between the waveguide and the cladding. The index difference was calculated by determination of the value of the input angle where the light disappeared from the screen (5) using the relation:

$$\sin \theta = n\sqrt{2\delta}, \quad (1)$$

where θ is the aperture angle, n is the refraction index of the cladding and δ is the refractive index variation between the waveguide and the surrounding cladding (unexposed region).

The linear absorption spectra were measured by utilizing a monochromator equipped with an optical multi-channel analyzer. A xenon lamp was used as a light source. After magnifying the sample mounted on an x – y – z translation stage by a mi-

croscope objective with numerical aperture of 0.4, the cladding region (unexposed area) or core region (photo-induced effect location) was blocked by an iris diaphragm. Therefore only the light transmitted through core (or cladding) region was registered. The selected area was imaged onto the entrance slit of the monochromator so that the linear absorption of the core or cladding could be obtained separately. The optical system allowed to measure the absorption spectra corresponding to an aperture diameter less than 5 μm .

Bulk glass samples of $\text{As}_{36}\text{S}_{64}$, $\text{As}_{40}\text{S}_{60}$ and $\text{As}_{42}\text{S}_{58}$ were used as reference samples in the study. Raman spectra of these samples were obtained prior to and following high power density He–Ne laser exposure. Spectra were recorded with a Labran confocal micro-Raman instrument from DILOR (typical resolution of $1\text{--}2\text{ cm}^{-1}$), in backscattering geometry at room temperature. The system consists of a holographic notch filter for Rayleigh rejection, a microscope equipped with $10\times$, $50\times$ and $100\times$ objectives (the latter allowing a spatial resolution of less than 2 μm), and CCD detector.

The sources used for illumination were either the 632.8 nm line of a He–Ne laser or the 752.5 nm line of a Kr laser. At first, a He–Ne laser with an output power of 10 mW was used, and the beam was focussed by means of the $10\times$ objective. Power density at the sample was estimated at 10^4 W/cm^2 . Under these conditions, we observed for all samples that illumination for a few tens of seconds produced the well-known photo-induced darkening effect. It was verified that an incident power density as low as $\cong 50\text{ W/cm}^2$ (laser output of 50 μW) was necessary to avoid any visible photo-darkening effect at this wavelength, during

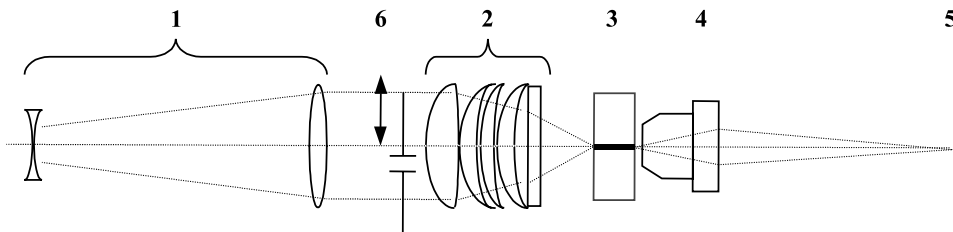


Fig. 1. Refractive index variation measurement set up by the aperture-angle method.

the experiment. A two-dimensional spatial map of Raman intensity ($15\ \mu\text{m} \times 15\ \mu\text{m}$ by a step of $1\ \mu\text{m}$ using a $100\times$ microscope objective) of the waveguide section of about $5\ \mu\text{m}$ diameter was recorded, using the $752.5\ \text{nm}$ exciting line (i.e., away from the glass absorption band in the transparent region) with an incident power of $80\ \mu\text{W}$. The cylindrical axis of the waveguide was oriented to be collinear with the optical microscope axis. The focus of the beam probing the waveguide section examined was situated inside the sample, $15\ \mu\text{m}$ below the surface.

3. Results

3.1. Waveguide writing in the bulk of $\text{As}_{40}\text{S}_{60}$ glass

The train of $\lambda = 850\ \text{nm}$ femtosecond pulses produced a uniform channel within the bulk of the glass samples. The diameter of the written waveguides was determined not only by the spot size of the focussed beam and the energy, but also by the speed of sample translation during writing. The slower translation speed led to the larger resulting waveguide diameter. Waveguides with diameters from the several microns up to $40\ \mu\text{m}$ were written. Fig. 2 illustrates optical micrographs of waveguides recorded in $\text{As}_{40}\text{S}_{60}$ glass samples. One can

see that these waveguides look like melted channel in glass samples. However, approximate evaluations of linear absorbed energy have shown that it was 10–50 times less than energy needed for melting in these glasses. These evaluations were verified experimentally. The laser used for writing could be used in a stable cw mode with the same or higher average power, but in this condition of operation, the waveguide recording ceased even when the average power was increased to nearly $1\ \text{W}$, that is three times more than in the case of femtosecond pulse generation. This phenomenon illustrates the intensity dependence of the waveguide writing and shows that just nonlinear effects can be responsible for additional absorption and extra heating of glasses.

The photo-induced structure created in the writing process disappears after a thermal treatment of 2 h at 25°C below the glass transition temperature, and the channel was no longer visible by the optical microscope. This observation is in agreement with the previous description of the reversible photo-induced effect observed in chalcogenide glasses [12]. Accurate determination of the aperture angle for guiding allowed an estimation of the index variation Δn between the waveguide and the cladding (Fig. 1). An index increase (Δn) of $5 \times 10^{-4} \pm 20\%$ was calculated from Eq. (1) in our samples. The transmission

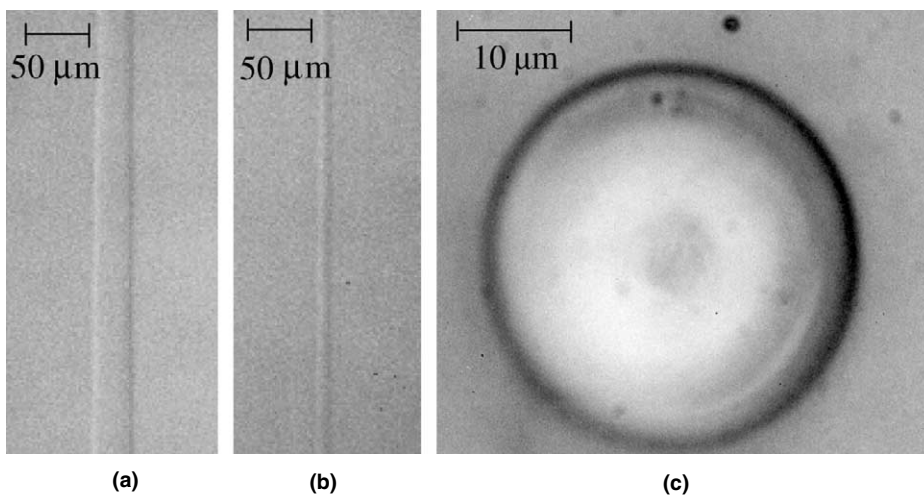


Fig. 2. Micrographs of the waveguide structure, (a) lateral view of waveguide, diameter $\sim 32\ \mu\text{m}$; (b) lateral view of waveguide, diameter $\sim 9\ \mu\text{m}$; (c) front view of waveguide, diameter $\sim 32\ \mu\text{m}$.

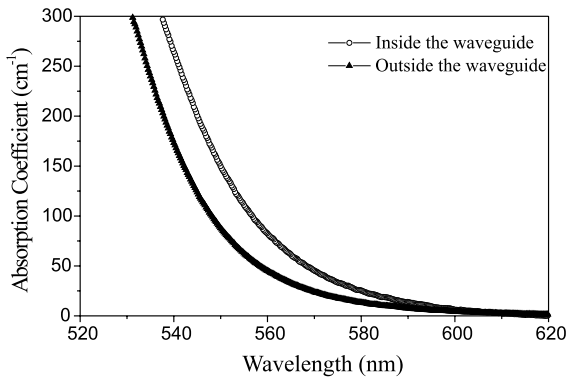


Fig. 3. Absorption coefficient of the $\text{As}_{40}\text{S}_{60}$ of the core of the waveguide (exposed region) and of the cladding (unexposed region).

spectra of the core of waveguide (exposed region) of 10 μm diameter and of the cladding (unexposed region) are shown in Fig. 3. The measurement shows a 15 nm red shift of the band gap that corresponds, according to the Kramer–Kronig relation, to the refractive index variation observed. The absorption spectra corresponding to the surrounding area of the waveguide (up to 10 μm from the waveguide) also exhibit a slight red shift of the optical gap, but smaller in magnitude (<5 nm). Such shift could be attributable to the mechanical stress induced following the extra heating and sharp quenching of channels during the waveguide formation process.

3.2. Structural analysis of the reference glasses

Raman spectra recorded in the bulk of glasses for the $\text{As}_{36}\text{S}_{64}$, $\text{As}_{40}\text{S}_{60}$ and $\text{As}_{42}\text{S}_{58}$ compositions are shown in Fig. 4 as well as the spectra recorded after exposure to a high power density (10^4 W/cm^2) 632.8 nm beam. The source used for illumination was the 632.8 nm line of a He–Ne laser. These spectra were used as reference for comparison to Raman spectra obtained for the waveguide structures prepared above. The Raman spectra corresponding to the different glass compositions are in accordance with those reported previously [14–18]. In all glasses the broad band centered at 345 cm^{-1} is characteristic of As–S vibrations in As– $\text{S}_{3/2}$ pyramidal sites. Vibrations

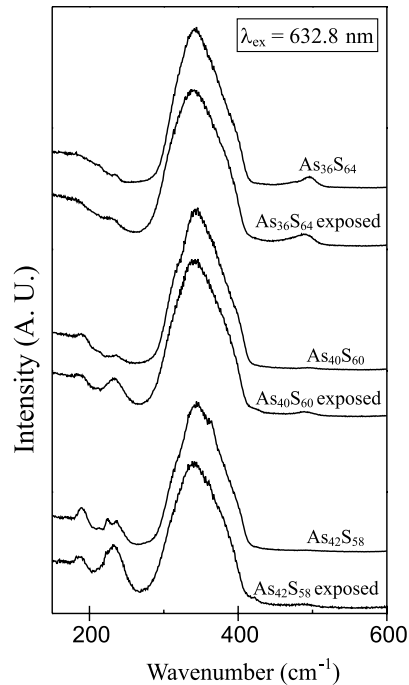


Fig. 4. Raman spectra of the glass composition $\text{As}_{36}\text{S}_{64}$, $\text{As}_{40}\text{S}_{60}$, $\text{As}_{42}\text{S}_{58}$ exposed and unexposed to high power density 632.8 cw laser.

of homopolar As–As and S–S bonds have been attributed to vibration bands at 168, 189, 223, 236, and 495 cm^{-1} , respectively. The bands at 155, 234, 474 cm^{-1} have been assigned to vibrations of S_8 rings [14,15]. Fig. 4 shows for the glass $\text{As}_{36}\text{S}_{64}$ two bands at 474 and 494 cm^{-1} related to the presence of S–S bonds as previously reported for excess sulfur glasses [15]. In addition to the band at 345 cm^{-1} , $\text{As}_{40}\text{S}_{60}$ glass also exhibits two weak bands centered at 236 and 494 cm^{-1} that can be attributed, respectively, to “wrong As–As and S–S chemical bonds” which should not be present in stoichiometric materials [10]. In the Raman spectrum of an arsenic-excess $\text{As}_{42}\text{S}_{58}$ glass, the bands at 189, 223 and 236 cm^{-1} attributed to As–As bonds are well defined. Two other bands are present, a weak band at 494 cm^{-1} that could be attributed again to “wrong” S–S bonds and a band at 362 cm^{-1} that was observed also by Wagner [15], but not assigned. S–S bonds in such a sulfur-deficient glass would not be expected.

No significant change in the Raman spectrum of the $\text{As}_{36}\text{S}_{64}$ glass was observed following exposure to high intensity 632.8 nm laser light (Fig. 4). It can be seen for the $\text{As}_{42}\text{S}_{58}$ glass that two clearly resolved bands at 223 and 236 cm^{-1} tend to merge into a broad band. This observation is consistent with the conclusions of Tanaka [19] who characterized a photo-induced darkening by an increase in randomness of the disordered network, which would most likely result in a broader distribution of bond distances and angles, which correspondingly would broaden the peaks in a Raman spectrum. In the spectrum of the glass $\text{As}_{40}\text{S}_{60}$ the intensity of the band at 236 cm^{-1} increases significantly and this effect is believed to be correlated to an increase in number of “As–As wrong bonds”, with laser exposure. The broadening of this band can be associated to the increase of the disorder of the glass structure. The band at 494 cm^{-1} shows a slight increase also, leading to the conclusion that new laser-induced S–S bonds are formed with exposure. This result would be expected if initially present As–S bonds are ruptured and rearranged to form As–As and S–S bonds.

3.3. Analysis of bulk glass waveguide

The Raman spectra recorded in the center of the waveguide, and far from the exposed region, are shown in Fig. 5. The source used for illumination

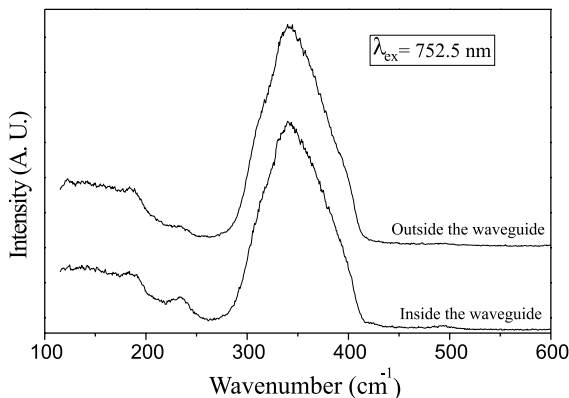


Fig. 5. Raman spectra of $\text{As}_{40}\text{S}_{60}$ of the core of the waveguide (exposed region) and of the cladding (unexposed region).

was the 752.5 nm line of a Kr laser. The spectrum of the unexposed region is in accordance with the spectra previously discussed for $\text{As}_{40}\text{S}_{60}$. The broad band at 345 cm^{-1} is present together with very weak bands located at 236 and 494 cm^{-1} indicating that our stoichiometric glass contains small numbers of wrong As–As and S–S bonds. The spectrum corresponding to the center (exposed core) of the waveguide exhibits the same three bands, but those at 236 and 494 cm^{-1} are markedly increased in intensity, while the band centered at 345 cm^{-1} shows a measurable decrease in intensity. A three-dimensional spatial Raman cartogram of the exposed region of the waveguide shown in Fig. 6 illustrates the spatial evolution of the intensity of the bands at 236 (Fig. 6(a)) and 345 cm^{-1} (Fig. 6(b)). Spectra were obtained from the plane perpendicular to the axis of the waveguide when focusing the laser beam 15 μm below the surface in order to minimize the influence of surface imperfections. This figure shows clearly an

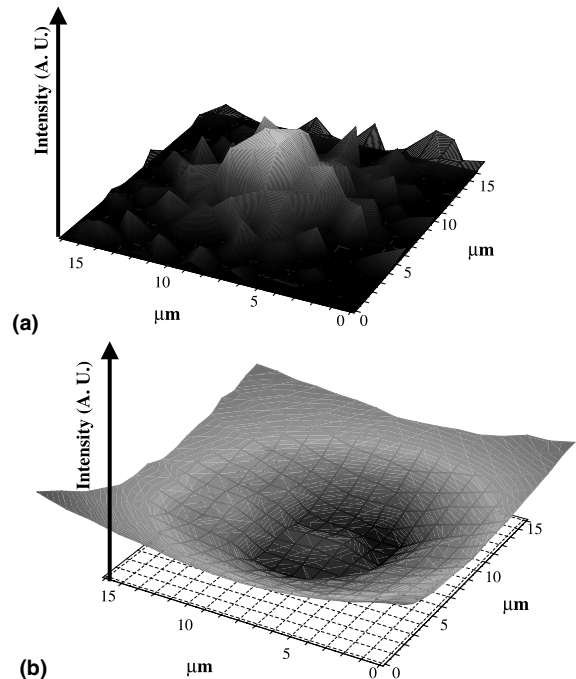


Fig. 6. Cartogram of the evolution of the Raman bands centered at 236 cm^{-1} (a) and at 345 cm^{-1} (b) of the section of the waveguide.

increase of the band centered at 236 cm^{-1} with the corresponding depletion in the As–S band at 345 cm^{-1} . It is worth noting however that the apparent depletion of the band at 345 cm^{-1} in Fig. 6(b) may be influenced by mechanical strains at the waveguide entrance which could slightly modify the optical path and the corresponding scattered intensity detected during the Raman measurement. However, this effect cannot explain the increase of the band centered at 236 cm^{-1} compared to the band at 345 cm^{-1} . Hence, according to these results, the photo-induced modification of chalcogenide glass at the local atomic scale is resulted from a breakage of some As–S bonds and the simultaneous formation of As–As and S–S chemical bonds during the laser writing process. This should lead to an increase of the randomness or disorder within the glass structure. This is consistent with the suggestion that in the As–Se glass system possessing an iso-structural glass network with As–S glasses and similar photo-darkening behavior, the photo-induced darkening is related to electronic states associated with As–As bonds close to the top of the “glass valence band” [20]. Pfeiffer et al. [12] noted that the local environment modification could not alone explain the photo-darkening effect. The increase of the randomness of the glass’ intermediate range order (IRO) should be considered for a complete understanding and validation of this conclusion.

A possible mechanism for the nonlinear absorption of laser radiation in chalcogenide glasses may be connected either with a spectral broadening of the femtosecond pulses within the glass medium or with a two-photon absorption process. The first phenomenon was observed in a series of silicate glasses [21]. It was shown that a photo-ionization of glasses having intrinsic absorption boundary in region of 230 nm could result from absorption of the short-wavelength component of the supercontinuum that was generated in the glass volume as a result of the femtosecond laser ($\lambda = 850\text{ nm}$) pulses spectral broadening. In our case this broadening could extend to the band edge of the electronic gap and leads to a strong linear absorption, and so to a photo-induced modification of glass structure. This is in agreement with the fact that the photo-induced effects were seen

for two kinds of high power density lasers, a cw laser at 632.8 nm and a femtosecond laser at 850 nm. Both of them had rather strong absorption in region of intrinsic absorption boundary of used glasses resulting for the first case from residual linear absorption, and for the second case from wide spectral broadening of laser pulses.

Another possible mechanism to describe the waveguide writing process is a two-photon absorption process. Significant two-photon absorption in chalcogenide glasses had been measured by different authors for excitation wavelength in the near infra-red [22,23]. Two-photon absorption could take place at a wavelength in the band gap of the material. It should be indicated that such mechanism has already been previously proposed by Meneghini et al. [3] to explain the formation of self-written waveguides in $\text{As}_{40}\text{S}_{60}$ films along the optical axis of a 800 nm femtosecond laser beam.

Thus, the question about real mechanism of nonlinear absorption is still open and demands separate study.

4. Conclusions

Waveguide structures were written using a train of femtosecond pulses at 850 nm in $\text{As}_{40}\text{S}_{60}$ glasses. A breakage of As–S bonds with formation of As–As and S–S bonds and an increase of the disorder of the glass structure leading to a photo-modification of glass optical properties were observed using Micro-Raman spectroscopy. These results were verified by comparison with reference arsenic-rich, and sulfur-rich glasses which contained the resulting bonds. The resulting index difference between the core (exposed) and surrounding cladding (unexposed) regions has been measured to be increased ($\Delta n = 5 \times 10^{-4}$) which was consistent with index changes seen in self-written planar waveguides written in the same material. Similarities in resulting photo-induced structural modification between band gap exposure and high intensity sub-band gap exposure have been shown. Two mechanisms of nonlinear absorption have been discussed as the origin of the chemical changes during waveguide formation. The structural change produced may prove to be very

promising for the control and the optimization of the waveguide writing procedure.

Acknowledgements

The authors would like to thank the group of Dr. Alain Villeneuve for useful discussions. We also acknowledge the assistance of Dr. George I. Stegeman and his group for many valuable discussions. This work was carried out through support from the University of Central Florida, CREOL, a Collaborative Grant from the NSERC (Natural Science and Engineering Research Council) of Canada, and DRET (France) grant number 93.811.00.091.

References

- [1] E.N. Glezer, M. Milosavljevic, L. Huang, R.J. Finlay, T.H. Her, J.P. Callan, E. Mazur, *Opt. Lett.* 21 (24) (1996) 2023.
- [2] K. Miura, J. Qiu, H. Inouye, T. Mitsuyu, *Appl. Phys. Lett.* 71 (23) (1997) 3329.
- [3] C. Meneghini, A. Villeneuve, *J. Opt. Soc. Am. B* 15 (12) (1998) 2946.
- [4] S.R. Elliott, *J. Non-Cryst. Solids* 81 (1987) 71.
- [5] S. Ramachandran, S.G. Bishop, J.P. Guo, D.J. Brady, *IEEE Phot. Tech. Lett.* 8 (8) (1996) 1041.
- [6] A. Zakery, P.J.S. Owen, A.E. Owen, *J. Non-Cryst. Solids* 198–200 (1996) 769.
- [7] T.V. Glastian, J.F. Viens, A. Villeneuve, M.A. Duguay, K. Richardson, *J. Lightwave Technol.* 15 (8) (1997) 1343.
- [8] K. Tanaka, *Solid State Commun.* 15 (1974) 1521.
- [9] R.A. Street, *Solid State Commun.* 24 (1977) 363.
- [10] C.Y. Yang, M.A. Paesler, D.E. Sayers, *Phys. Rev. B* 36 (17) (1987) 9160.
- [11] L.F. Gladden, S.R. Elliott, G.N. Greaves, *J. Non-Cryst. Solids* 106 (1998) 189.
- [12] G. Pfeiffer, M.A. Paesler, S.C. Agarwal, *J. Non-Cryst. Solids* 130 (1991) 111.
- [13] J.-F. Viens, C. Meneghini, A. Villeneuve, T. Galstian, E.J. Knystautas, M.A. Duguay, K.A. Richardson, T. Cardinal, *J. Lightwave Technol.* 17 (7) (1999) 1184.
- [14] A.T. Ward, *J. Phys. Chem.* 72 (1968) 4133.
- [15] T. Wagner, S.O. Kasap, M. Vlcek, A. Sklenar, A. Stronski, *J. Non-Cryst. Solids* 227–230 (1998) 752.
- [16] J.A. Freitas Jr., U. Strom, D.J. Treacy, *J. Non-Cryst. Solids* 59–60 (1983) 875.
- [17] T. Cardinal, K. Richardson, H. Shim, A. Schulte, R. Beatty, K. Le Foulgoc, C. Meneghini, J.F. Viens, A. Villeneuve, *J. Non-Cryst. Solids* 256–257 (1999) 353.
- [18] M. Frumar, Z. Polak, Z. Cernosek, *J. Non-Cryst. Solids* 256–257 (1999) 105.
- [19] K. Tanaka, *J. Non-Cryst. Solids* 35–36 (1980) 1023.
- [20] P. Krecmer, M. Vlcek, S.R. Elliot, *J. Non-Cryst. Solids* 227–230 (1998) 682.
- [21] O.M. Efimov, L.B. Glebov, S. Grantham, M. Richardson, *J. Non-Cryst. Solids* 253 (1999) 58.
- [22] R. Rangel-Rojo, T. Kosa, E. Hajto, P.J.S. Ewen, A.E. Owen, A.K. Kar, B.S. Wherrett, *Opt. Commun.* 109 (1994) 145.
- [23] K.A. Cerqua-Richardson, J.M. McKinley, B. Lawrence, S. Joshi, A. Villeneuve, *Opt. Mater.* 10 (1998) 155.